

THE ONSET AND DECONFINEMENT TRANSITIONS IN TWO-COLOUR QCD

*Jon-Ivar Skullerud*¹, *Simon Hands*² and *Seyong Kim*^{2,3}

¹School of Mathematics, Trinity College, Dublin 2, Ireland

²Department of Physics, University of Wales Swansea, Singleton Park, Swansea SA2 8PP, UK

³Department of Physics, Sejong University, Gunja-Dong, Gwangjin-Gu, Seoul 143-747, South Korea

Abstract

We study two-colour QCD with two flavours of Wilson fermion at non-zero chemical potential μ and zero temperature. We find evidence of two separate transitions: an onset transition at $\mu \approx m_\pi/2$ where quark number and energy densities increase from zero; and a deconfinement transition at higher μ . The μ -dependence of the number and energy densities and the diquark condensate indicate that a Fermi surface is formed and that BCS rather than Bose–Einstein condensation dominates at the quark mass considered here, especially beyond the deconfinement transition.

1 Introduction

QCD with gauge group $SU(2)$ and non-zero chemical potential μ has a number of features that makes it an interesting object of study. Since the quarks and antiquarks live in equivalent representations of the colour group and can be related by an anti-unitary symmetry (the Pauli–Gürsey symmetry), the fermion determinant remains real at non-zero μ . For an even number of flavours, it can also be shown to be positive, making standard Monte Carlo sampling possible. Thus two-colour QCD can be used as a laboratory for investigating gauge theories at high density and low temperature, a region of phase space which is still inaccessible to lattice simulations of real (three-colour) QCD.

At $\mu = 0$, the Pauli–Gürsey symmetry implies an exact symmetry between mesons and diquarks, which are the baryons of the theory. In particular, chiral multiplets will contain both mesons and baryons. For $N_f = 2$ for example, the pseudo-Goldstone multiplet consists of the pion isotriplet plus a scalar isoscalar diquark–antidiquark pair. The diquarks can be expected to condense when $\mu \gtrsim m_\pi/2$, forming a superfluid ground state. In this respect, the theory is radically different from real QCD, where no gauge invariant diquark condensate exist and the ground state at high density is superconducting. The nature of the superfluid ground state is however an interesting issue in its own right.

When $m_\pi \ll m_\rho$ (ρ denoting any non-Goldstone boson) the μ -dependence of the theory can be analysed using chiral perturbation theory [1]. In this case a transition to a Bose–Einstein condensate (BEC) of tightly bound diquarks occurs at $\mu = \mu_o = m_\pi/2$, giving rise to a quark density n_q and diquark condensate $\langle qq \rangle$,

$$n_q \propto f_\pi^2(\mu - \mu_o); \quad \langle qq \rangle \propto \sqrt{1 - \left(\frac{\mu_o}{\mu}\right)^4} \Rightarrow \lim_{\mu \rightarrow \infty} \langle qq(\mu) \rangle = \text{const.} \quad (1)$$

This has been confirmed in simulations with staggered fermions [2, 3, 4, 5].

This picture is expected to break down when $m_\pi \approx m_\rho$, at which point the Goldstones are no longer distinguished hadrons, and the fermionic nature of the constituents comes into play. At this point one may expect BCS condensation of quarks near the Fermi surface to become the dominant mechanism. Assuming states within thickness $\Delta \ll \mu$ around the Fermi surface participate in the pairing, we obtain the following qualitative behaviour:

$$n_q \propto \mu^3; \quad \langle qq \rangle \propto \Delta \mu^2. \quad (2)$$

The same rule of thumb predicts the quark energy density $\varepsilon_q \propto \mu^4$.

In the gluon sector, the differences between SU(2) and SU(3) are expected to be less important, and 2-colour QCD is a good setting for *ab initio* studies of gluodynamics in the presence of a background baryon density. Of particular interest is the issue of deconfinement at high density. Signals of deconfinement were observed in simulations with Wilson [6] and staggered fermions [7], where correlations were found between the Polyakov loop and chiral or baryonic observables. However, the phase structure has not been investigated in any further detail, and it remains unclear whether there is a confined phase with non-zero baryon number (as in QCD), or just a single phase transition. This will be investigated in the present paper.

2 Lattice formulation

The $N_f = 2$ fermion action is given by

$$S = \bar{\psi}_1 M(\mu) \psi_1 + \bar{\psi}_2 M(\mu) \psi_2 - J \bar{\psi}_1 (C\gamma_5) \tau_2 \bar{\psi}_2^{tr} + \bar{J} \psi_2^{tr} (C\gamma_5) \tau_2 \psi_1, \quad (3)$$

where $M(\mu)$ is the usual Wilson fermion matrix

$$M_{xy}(\mu) = \delta_{xy} - \kappa \sum_{\nu} [(1 - \gamma_{\nu}) e^{\mu\delta_{\nu 0}} U_{\nu}(x) \delta_{y, x+\hat{\nu}} + (1 + \gamma_{\nu}) e^{-\mu\delta_{\nu 0}} U_{\nu}^{\dagger}(y) \delta_{y, x-\hat{\nu}}]. \quad (4)$$

The diquark source terms J, \bar{J} serve a double purpose in lifting the low-lying eigenmodes in the superfluid phase, thus making the simulation numerically tractable, and enabling us to study diquark condensation without any ‘‘partial quenching’’. The results will at the end be extrapolated to the physical limit $J = \bar{J} = 0$. We will also introduce the rescaled source strength $j \equiv J/\kappa$.

The Pauli–Gürsey symmetry is

$$KM(\mu)K^{-1} = M^*(\mu) \quad \text{with} \quad K \equiv C\gamma_5\tau_2. \quad (5)$$

This symmetry implies that $\det M(\mu)$ is real, but not necessarily positive. However, with the change of variables $\bar{\phi} = -\psi_2^{tr} C\tau_2, \phi = C^{-1}\tau_2\bar{\psi}_2^{tr}$ we can rewrite the action as

$$S = (\bar{\psi} \quad \bar{\phi}) \begin{pmatrix} M(\mu) & J\gamma_5 \\ -\bar{J}\gamma_5 & M(-\mu) \end{pmatrix} \begin{pmatrix} \psi \\ \phi \end{pmatrix} \equiv \bar{\Psi} \mathcal{M} \Psi. \quad (6)$$

It is now straightforward to show that $\det \mathcal{M}$ is real and positive if $\bar{J} = J^*$ [8, 9], and it is possible to simulate this action with a standard HMC algorithm [9].

We have computed the quark number and energy densities, diquark condensate, gluon energy density and Polyakov loop on each trajectory. The quark number density is given by

$$n_q = \sum_i \kappa \left\langle \bar{\psi}_i(x) (\gamma_0 - 1) e^{\mu} U_t(x) \psi_i(x + \hat{t}) + \bar{\psi}_i(x) (\gamma_0 + 1) e^{-\mu} U_t^{\dagger}(x - \hat{t}) \psi_i(x - \hat{t}) \right\rangle. \quad (7)$$

The energy density is given by

$$\varepsilon_q = \sum_i \kappa \left\langle \bar{\psi}_i(x) (\gamma_0 - 1) e^{\mu} U_t(x) \psi_i(x + \hat{t}) - \bar{\psi}_i(x) (\gamma_0 + 1) e^{-\mu} U_t^{\dagger}(x - \hat{t}) \psi_i(x - \hat{t}) \right\rangle - \varepsilon_q^0, \quad (8)$$

where the vacuum subtraction ε_q^0 is

$$\varepsilon_q^0 = \frac{4}{d} \left(N_f N_c - \langle \bar{\psi} \psi \rangle_{\mu=0} \right). \quad (9)$$

The diquark condensate is

$$\langle qq \rangle = \frac{\kappa}{2} \langle \bar{\psi}_1 K \bar{\psi}_2^{tr} - \psi_2^{tr} K \psi_1 \rangle, \quad (10)$$

while the gluon energy density is given by $\varepsilon_g = \frac{3\beta}{2} \langle \text{Tr}(P_t - P_s) \rangle$, where P_t and P_s are the timelike and spacelike plaquettes respectively.

3 Results

We have simulated with $\beta = 1.7, \kappa = 0.178$ on an $8^3 \times 16$ lattice, corresponding to $a = 0.22$ fm, $m_\pi/m_\rho = 0.92$ [10]. We have used a diquark source $a_j = 0.04$ with $0.3 \leq a\mu \leq 1.0$. The number of trajectories and their length are given in table 1. We have also started simulations for selected values of μ with $a_j = 0.02$, but those results will not be shown here. Configurations were saved every 4 trajectories of length 1 and every 8 trajectories of length 0.5.

In figure 1 we show results for the Polyakov loop, gluon and quark energy densities, quark number density and diquark condensate, as function of chemical potential. We see evidence of two distinct transitions: first, an *onset* transition around $a\mu = 0.4$ where the quark number and energy density increase from zero; and second, a *deconfinement* transition around $a\mu = 0.65$ where the Polyakov loop takes on a non-zero value. We also find that the chiral condensate starts to decrease from its vacuum value around $a\mu = 0.4$.

The behaviour of n_q and $\langle qq \rangle$ appears strikingly different from that of (1), and is suggestive of the formation of a Fermi surface and a μ -dependence qualitatively similar to that of (2) [9]. On the coarse lattices used here, the continuum behaviour may however be obscured by lattice artefacts. To compensate for this, we divide our results with the expected behaviour of free, massless Wilson fermions on an $N_s^3 \times N_t$ lattice,

$$n_{q,\text{free}} = \frac{4N_f N_c}{N_s^3 N_t} \sum_k \frac{i \sin \tilde{k}_0 [\sum_i \cos k_i - 4]}{[4 - \sum_\nu \cos \tilde{k}_\nu]^2 + \sum_\nu \sin^2 \tilde{k}_\nu} \quad (11)$$

where

$$\tilde{k}_\nu = \begin{cases} k_0 - i\mu = \frac{2\pi}{N_t} (n_0 + \frac{1}{2}) - i\mu, & \nu = 0, \\ k_\nu = \frac{2\pi n_\nu}{N_s}, & \nu = 1, 2, 3. \end{cases} \quad (12)$$

and $N_s = 8, N_t = 16$ in our case. The result of this is shown in figure 2. The number density shows good BCS scaling already from $a\mu \approx 0.5$, while no such agreement is shown for the energy density until the deconfinement transition. The fact that n_q exceeds the free field value by a factor of two is consistent with a degenerate system with $k_F > E_F$, suggesting a non-zero binding energy. Strikingly, the gluon energy density exhibits very good scaling with μ^4 over the whole range of μ considered.

Also in fig. 2, we show the diquark condensate divided by μ^2 , which should be constant in the case of BCS condensation. Such scaling is indeed observed in the deconfined phase, for $a\mu \gtrsim 0.65$. Below this point the behaviour appears to be in qualitative agreement with the χ PT expression (1), but this requires further study before any firm conclusion can be drawn.

Finally, in figure 3 we show the static quark potential for selected values of μ . We see clear evidence of screening for $a\mu \geq 0.4$. However, for $a\mu \gtrsim 0.7$ a new pattern appears to emerge, in that the short-distance potential is strongly modified (and suppressed) while the long-distance screening, if anything, is reversed. This is most clearly seen in the right-hand plot of fig. 3, where the deviation of the potential from that at $\mu = j = 0$ is shown. The source of this behaviour is subject of ongoing investigation.

4 Discussion

We have studied the μ -dependence of local observables and the static quark potential for 2-colour QCD with a quark mass well beyond the expected range of validity for chiral perturbation theory. We find clear

$a\mu$	$N(\ell = 0.5)$	$N(\ell = 1.0)$
0.3	300	
0.35		230
0.4	300	90
0.45	300	64
0.5	300	42
0.55	300	
0.6	303	108
0.65		288
0.7	302	48
0.75		137
0.8	280	58
0.9	300	
1.0	300	

Table 1: Run parameters for the HMC simulations. N is the number of trajectories, while ℓ is the average trajectory length.

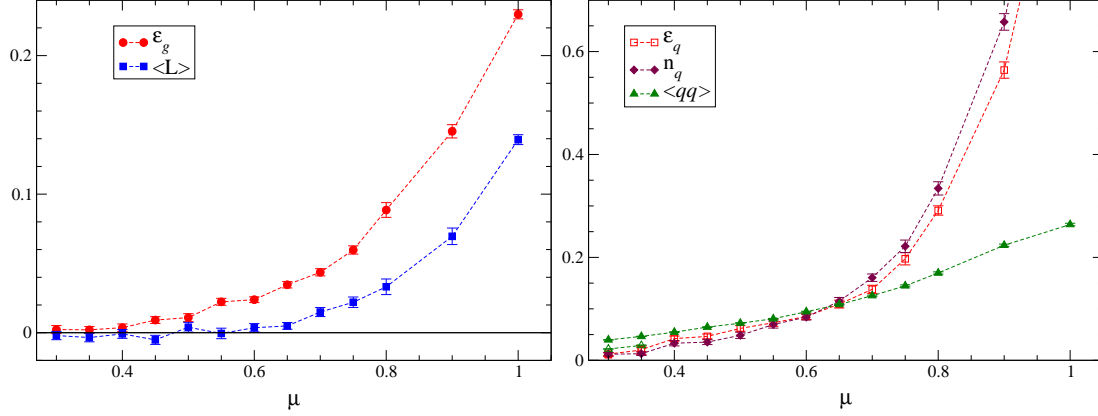


Fig. 1: Results for bosonic (left) and fermionic (right) quantities, as a function of chemical potential μ , for $a_j = 0.04$. The open triangles are preliminary results for the diquark condensate with $a_j = 0.02$.

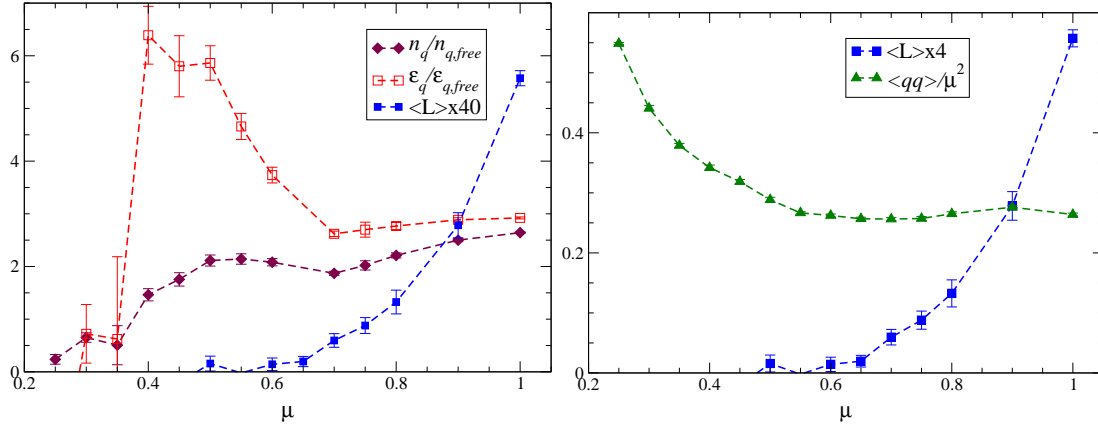


Fig. 2: Left: Quark number density n_q and energy density ε_q , divided by their values for free massless fermions on an $8^3 \times 16$ lattice. Right: The diquark condensate $\langle qq \rangle$ divided by the BCS formula (2), together with the average Polyakov loop $\langle L \rangle$.

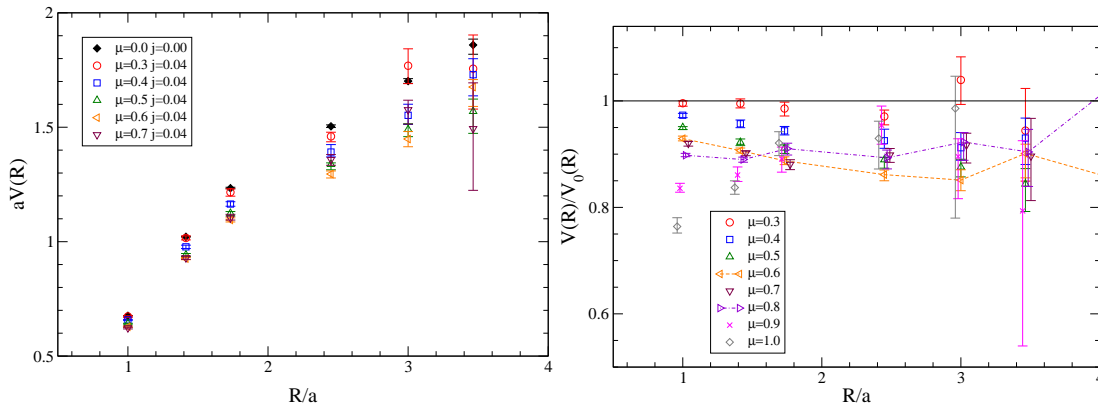


Fig. 3: The static quark potential for different values of the chemical potential μ . The right-hand plot shows the potential normalised to its value at $\mu = j = 0$.

evidence of two separate (onset and deconfining) transitions, and strong indications that a Fermi surface is formed, leading to the formation of a BCS condensate at high densities. In this sense, the system is more QCD-like than 2-colour QCD at lighter quark masses, where BEC dominates.

The simulations have been carried out with a fixed, non-zero diquark source j . We are currently performing simulations with a second, smaller diquark source to enable an extrapolation to $j = 0$. This will lay the grounds for drawing more definite conclusions regarding the nature of the system in the different regions.

We are also studying the electric and magnetic gluon propagator, which may provide useful input into the gap equation at high densities, and are planning to study the hadron spectrum, focusing in particular on the fate of the vector meson, which in a previous study [6] was found to become lighter at higher density.

Acknowledgments

This work has been supported by the IRCSET Embark Initiative award SC/03/393Y. SK thanks PPARC for support during his visit to Swansea in 2004/05. SJH was supported by a PPARC Senior Research Fellowship. We have benefited from discussions with Kim Splittorff and Jimmy Juge, and give our warm thanks to Shinji Ejiri and Luigi Scorzato for their participation in the early stages of this project.

References

- [1] J. Kogut et al., Nucl. Phys. B582 (2000) 477 [hep-ph/0001171].
- [2] R. Aloisio et al., Phys. Lett. B493 (2000) 189 [hep-lat/0009034].
- [3] S. Hands et al., Eur. Phys. J. C17 (2000) 285 [hep-lat/0006018].
- [4] S. Hands et al., Eur. Phys. J. C22 (2001) 451 [hep-lat/0109029].
- [5] J. Kogut et al., Phys. Rev. D64 (2001) 094505 [hep-lat/0105026].
- [6] S. Muroya, A. Nakamura and C. Nonaka, Phys. Lett. B551 (2003) 305 [hep-lat/0211010].
- [7] B. Allés et al., hep-lat/0210039.
- [8] J.I. Skullerud et al., Prog. Theor. Phys. Suppl. 153 (2004) 60 [hep-lat/0312002].
- [9] S. Hands, S. Kim and J.I. Skullerud, PoS (LAT2005) (2005) 149 [hep-lat/0508027].
- [10] J.I. Skullerud, Simulating SU(2)-QCD with Wilson fermions, 2004, http://mocha.phys.washington.edu/~int_talk/WorkShops/int_04_1/People/Skullerud_J/.